

Journal of Mechanics of Materials and Structures

AN ANALYTICAL SOLUTION FOR HEAT FLUX DISTRIBUTION OF
CYLINDRICALLY ORTHOTROPIC FIBER REINFORCED COMPOSITES
WITH SURFACE EFFECT

Junhua Xiao, Yaoling Xu and Fucheng Zhang

Volume 13, No. 4

July 2018



AN ANALYTICAL SOLUTION FOR HEAT FLUX DISTRIBUTION OF CYLINDRICALLY ORTHOTROPIC FIBER REINFORCED COMPOSITES WITH SURFACE EFFECT

JUNHUA XIAO, YAOLING XU AND FUCHENG ZHANG

A theoretical study is conducted on the problem of two-dimensional steady-state heat transfer of composites with cylindrically orthotropic fiber with surface effect containing isotropic core. By introducing an appropriate coordinate transformation to convert the governing differential equation into a harmonic one, an analytical solution to the heat flux fields of the cylindrically orthotropic nanofiber reinforced composites is derived based on the surface theory model. Numerical examples provide a better understanding of interesting interaction effects of composite microstructures (geometric and physical parameters of the fiber and core) in heat flux distribution. The radial and circumferential heat flux distributions in the nanocomposites are investigated. The effects of size of the fiber, thermal conductivity of the core and radius of the core on the heat flux distribution are discussed.

1. Introduction

Carbon fiber reinforced composites have been extensively used in modern industries including sports equipment, civil engineering, mechanical engineering, aerospace structures, defense and automobile industries [DeValve and Pitchumani 2013; Peng et al. 2017], because of their high specific strength, modulus, stiffness, low density, thermal stability, and corrosion resistance [Khan et al. 2010; Wang et al. 2012; Li et al. 2017]. Different from common fibers, carbon fibers exhibit special heterogeneity and anisotropy [Hashin 1990; Christensen 1994], that is, polyacrylonitrile based carbon fibers generally exhibit circumferential alignment of the graphite basal planes, and pitch based carbon fibers typically show radial alignment [Yan et al. 2010; Avery and Herakovich 1986; Knott and Herakovich 1991].

Thermal performance is one of the most important properties of composites in many applications as thermal protections, heat shields and heat guides [Gori and Corasaniti 2014]. In recent years, significant progress has been made in addressing the effective thermal conductivity of composites from a fundamental perspective by using theoretical, numerical and experimental methods.

The knowledge of heat flux fields is also important to understanding and predicting the thermal properties of composite in many heat conduction problems [Frankel et al. 2008; Stokes-Griffin and Compston 2016]. The heat flux distribution in composites is a basilica problem in inverse heat transfer problem [Alifanov 1994; Orlande 2011]. The following are some representative literatures in recent years. By presenting a finite element model, Rodríguez and Cabeza [1999] investigated the heat flux distribution in a composite with cylindrically orthotropic and homogeneous fiber. Using a thermomechanical cohesive zone model, Hattiangadi and Siegmund [2005] studied the distribution of total heat flux drop ahead of the crack tip across an intact interface for different values of interface conductance. Based on the

Keywords: surface effect, nanofiber, size dependent, heat flux, cylindrically orthotropic fiber.

conjugate gradient method, Yang and Chang [2006] estimated the heat and moisture fluxes of a double-layer annular cylinder with interface resistance. Yin et al. [2008] derived the heat flux field for a single particle embedded in a graded material by using the equivalent inclusion method. Frankel et al. [2010] presented a new heat flux-temperature integral relationship for anisotropic materials and obtained both an exact analytic solution for temperature and heat flux. Yang et al. [2010] estimated the heat flux and temperature distributions for the system composed of a multilayer composite strip and semi-infinite foundation based on the conjugate gradient method and the discrepancy principle. Yan et al. [2010] examined the effects of the existence of the core and the cylindrical orthotropy of the fiber on the heat flux at the center of the fiber. Lee et al. [2012] developed an inverse analysis for simultaneously estimating the heat fluxes at the inner and outer boundary surfaces of a functionally graded hollow circular cylinder from the knowledge of temperature measurements taken within the cylinder. Shi et al. [2013] calculated the cold wall heat flux of silica-phenolic composite exposed to heat flux environments. Yang et al. [2013] solved the inverse hyperbolic heat conduction problem in estimating the inner-wall heat flux of a hollow cylinder from the knowledge of temperature measurements taken within the medium. Rylko [2015] presented the temperature distribution and the heat flux expressed in terms of a series in the radius of ideally conducting fibers in deterministic and random composites. Gounni and Alami [2017] studied the optimal allocation of the phase change material within a composite wall for surface temperature and heat flux reduction by an experimental approach.

To the best of our knowledge, the investigation on the distribution characteristics of the heat flux fields in the nanocomposites reinforced with cylindrically orthotropic fiber has not been reported. Classical heat transfer theory does not address size effect of the fibers in composites. However, size effect of the heat properties for nanocomposites often become prominent when the size of reinforced fibers are on the order of nanometer [Györy and Márkus 2014; Machrafı 2016; Sobolev 2017]. The surface effect of nanofibers plays an important role in heat flux fields in the nanocomposites because of the high surface-to-volume ratios of this solid material. By introducing interface physical constants, Gurtin-Murdoch surface theory [Gurtin and Murdoch 1975; Gurtin and Murdoch 1978; Gurtin et al. 1998] takes into account the nanoscale microresponse in the macroscopic response of the material, which has become an effective analytical method for studying microscopic and macroscopic properties of the nanocomposites. Duan and Karihaloo [2007] prove that when the thermoelastic term is included in the constitutive relation of interface stress model, there exists an exact relation between the effective coefficient of thermal expansion and the effective elastic moduli of the heterogeneous medium. Recent research [Xiao et al. 2018] shows that the surface theory model can be applied to solve the heat transfer problem of nanofiber reinforced composites.

This work investigates the heat flux distribution of composites reinforced with cylindrically orthotropic nanofiber under two dimensional steady-state heat transfer conditions. An analytical solution to the heat flux fields in the composites is derived by using the surface theory model. The effects of the fiber size, the core thermal conductivity and the core radius on the heat flux fields are discussed.

2. Model and complex variable elasticity theory

Consider a cylindrically orthotropic fiber with surface effect containing isotropic core under two dimensional steady-state heat conduction as shown in Figure 1, where (x, y) denotes the Cartesian coordinates

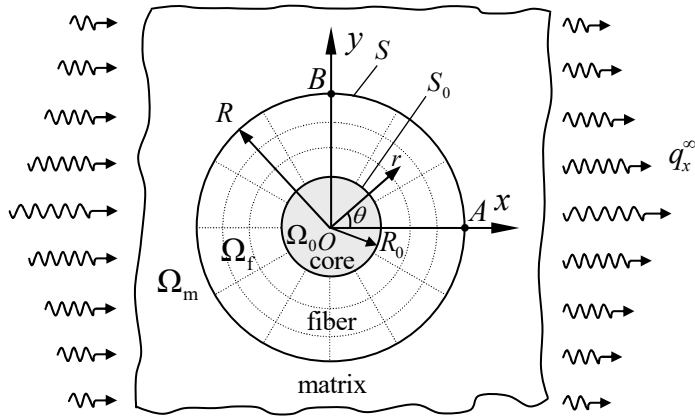


Figure 1. A cylindrically orthotropic fiber with surface effect containing isotropic core under far-field constant heat flux q_x^∞ .

and (r, θ) denotes the polar coordinates. Random orientation of the graphite basal planes in the transverse plane of the fiber would result in a transversely isotropic core in the carbon fiber [Avery and Herakovich 1986; Knott and Herakovich 1991], which is shown in the Figure. The regions Ω_0 , Ω_f , Ω_m denote the isotropic fiber core, the cylindrically orthotropic nanofiber and the isotropic matrix, respectively. The contour S with a radius R denotes the interface between the fiber and the matrix, which possesses different thermal property from the fiber and the matrix. The contours S_0 with a radius R_0 denote the interfaces between the fiber core and the fiber. The subscripts 0, f, m denote the fiber core, the fiber and the matrix, respectively. Assuming the nanocomposites is subjected to a far-field constant heat flux q_x^∞ along the x axis. Based on the theory of Gurtin–Murdoch surface model [Gurtin and Murdoch 1975; Gurtin and Murdoch 1978; Gurtin et al. 1998], the nanofiber interface S has its own thermal property, which is regarded as a layer without thickness [Xiao et al. 2018].

The basic equation of the problem can be given as

$$\frac{\partial q_r}{\partial r} + \frac{q_r}{r} + \frac{\partial q_\theta}{r \partial \theta} = 0 \quad \text{in } \Omega_0, \Omega_f, \Omega_m, \quad (1)$$

$$\begin{bmatrix} H_r \\ H_\theta \end{bmatrix} = \begin{bmatrix} \partial T / \partial r \\ \frac{1}{r} (\partial T / \partial \theta) \end{bmatrix} \quad \text{in } \Omega_0, \Omega_f, \Omega_m, \quad (2)$$

$$\begin{Bmatrix} q_r \\ q_\theta \end{Bmatrix} = - \begin{bmatrix} k_r & 0 \\ 0 & k_\theta \end{bmatrix} \begin{Bmatrix} H_r \\ H_\theta \end{Bmatrix} \quad \text{in } \Omega_f, \quad (3)$$

$$\begin{Bmatrix} q_r \\ q_\theta \end{Bmatrix} = - \begin{bmatrix} k_i & 0 \\ 0 & k_i \end{bmatrix} \begin{Bmatrix} H_r \\ H_\theta \end{Bmatrix} \quad (i = 0, m) \quad \text{in } \Omega_0, \Omega_m, \quad (4)$$

where q , H and T denote heat flux, temperature gradient and temperature, respectively; k_r and k_θ are the radial and circumferential conductivities, respectively.

By substituting (2) and (3) into (1) yields the following governing differential equation:

$$\frac{\partial}{\partial r} \left(r \frac{\partial T}{\partial r} \right) + \gamma^2 \frac{1}{r} \frac{\partial^2 T}{\partial \theta^2} = 0 \quad \text{in } \Omega_f, \tag{5}$$

where $\gamma = \sqrt{k_\theta/k_r}$. Define a complex plane z :

$$z = x + iy = r e^{i\theta}. \tag{6}$$

In general, $\gamma \neq 1$ (i.e. $k_r \neq k_\theta$), equation (5) is not a harmonic equation. Introduce a new complex plane z_1 as follows [Yan et al. 2010]

$$z_1 = r e^{i\theta_1}, \tag{7}$$

where $\theta_1 = \theta/\gamma$. In the z_1 -plane, equation (5) is transformed into a harmonic equation:

$$\frac{\partial}{\partial r} \left(r \frac{\partial T}{\partial r} \right) + \frac{1}{r} \frac{\partial^2 T}{\partial \theta_1^2} = 0. \tag{8}$$

The transformation from the z -plane to the z_1 -plane is not a conformal mapping. Introduce again a complex plane ζ as follows

$$\zeta = z_1^\gamma = r^{\gamma-1} z. \tag{9}$$

It is a conformal mapping from z -plane to plane ζ .

The temperature field T is a harmonic function in ζ -plane and can be expressed as an analytical function $\omega(\zeta)$:

$$T = \frac{1}{2} [\omega(\zeta) + \overline{\omega(\zeta)}] = \text{Re}[\omega(\zeta)]. \tag{10}$$

Define the heat transfer rate Φ along the arc \widehat{AB} :

$$\Phi = \frac{i}{2} \sqrt{k_r k_\theta} [\omega(\zeta) - \overline{\omega(\zeta)}]_A^B = -\sqrt{k_r k_\theta} \text{Im}[\omega(\zeta)]_A^B. \tag{11}$$

By substituting (10) into (2) and (3), it is the following expressions are obtained that

$$\begin{cases} q_r = -\frac{\gamma}{r} k_r \text{Re}[\omega'(\zeta)\zeta] \\ q_\theta = \frac{1}{r} k_\theta \text{Im}[\omega'(\zeta)\zeta] \end{cases} \quad \text{in } \Omega_f. \tag{12}$$

Then, equation (12) can be rewritten as

$$\frac{q_r}{\gamma k_r} - i \frac{q_\theta}{k_\theta} = -\frac{1}{r} \{ \text{Re}[\omega'(\zeta)\zeta] + i \text{Im}[\omega'(\zeta)\zeta] \} = -\frac{\zeta}{r} \omega'(\zeta) \quad \text{in } \Omega_f. \tag{13}$$

When $\gamma = 1$ (i.e. $k_r = k_\theta = k$), equations (11) and (13) degenerate into the following expressions:

$$\Phi = \frac{i}{2} k [\omega(\zeta) - \overline{\omega(\zeta)}]_A^B = -k \text{Im}[\omega(\zeta)]_A^B, \tag{14}$$

$$q_r - i q_\theta = -\frac{k}{r} \omega'(z) z, \tag{15}$$

$$q_x - i q_y = -k \omega'(z). \tag{16}$$

3. Exact solution to heat flux fields

On the interface S , the nonclassical heat transfer boundary conditions can be written as [Xiao et al. 2018]

$$q_r^f - q_r^m = \frac{1}{R} \frac{\partial q_\theta^S}{\partial \theta} \quad \text{on } S, \tag{17}$$

$$q_\theta^{S_1} = -k_s H_\theta^S \quad \text{on } S, \tag{18}$$

where k_s is the interface thermal constant.

For a coherent interface, the interfacial temperature gradient is equal to the associated temperature gradient in the abutting bulk materials, i.e.

$$H_\theta^S = H_\theta^f(R) = H_\theta^m(R). \tag{19}$$

Assuming the fiber-core interface S_0 is perfect and the fiber-matrix interface S is imperfect, the boundary conditions at the interfaces S_0 and S can be given as

$$T_0 = T_f \quad \text{on } S_0, \tag{20}$$

$$\Phi_0 = \Phi_f \quad \text{on } S_0, \tag{21}$$

$$T_f = T_m \quad \text{on } S, \tag{22}$$

$$q_r^f - q_r^m = -\frac{k_s}{R} \frac{\partial H_\theta^S}{\partial \theta} \quad \text{on } S. \tag{23}$$

In an annular region, the analytical function $\omega(z)$ can be expanded into Laurent series [Muskhelishvili 1953]:

$$\omega(z) = a^* \ln z + \sum_{k=-\infty}^{\infty} a_k z^k, \tag{24}$$

where a^* and a_k are complex constants to be determined.

The complex potential $\omega_0(z)$ and $\omega_m(z)$ are expanded in z -plane and the complex potential $\omega_f(\zeta)$ is expanded in ζ -plane. It is seen that taking the following finite terms of the series can arrive at the exact solution:

$$\omega_0(z) = A_1 z \quad \text{in } \Omega_0, \tag{25}$$

$$\omega_f(\zeta) = B_1 \zeta + B_{-1} \frac{1}{\zeta} = B_1 r^{\gamma-1} z + \frac{B_{-1}}{r^{\gamma-1}} \frac{1}{z} \quad \text{in } \Omega_f, \tag{26}$$

$$\omega_m(z) = C_1 z + C_{-1} \frac{1}{z} \quad \text{in } \Omega_m, \tag{27}$$

where $A_1, B_1, B_{-1}, C_1,$ and C_{-1} are constants to be determined.

Substituting (27) into (16) and integrating with the far field condition $(q_x^m - iq_y^m)|_{z \rightarrow \infty} = q_x^\infty - iq_y^\infty$, we obtain

$$C_1 = -\frac{q_x^\infty}{k_m}. \tag{28}$$

From (20)–(23), one obtains the following expressions:

$$A_1 = B_1 R_0^{\gamma-1} + \frac{B_{-1}}{R_0^{\gamma+1}}, \tag{29}$$

$$k_0 A_1 = \sqrt{k_r k_\theta} \left(B_1 R_0^{\gamma-1} - \frac{B_{-1}}{R_0^{\gamma+1}} \right), \tag{30}$$

$$B_1 R^{\gamma-1} + \frac{B_{-1}}{R^{\gamma+1}} = C_1 + \frac{C_{-1}}{R^2}, \tag{31}$$

$$k_m \left(C_1 - \frac{C_{-1}}{R^2} \right) - \gamma k_r \left(B_1 R^{\gamma-1} - \frac{B_{-1}}{R^{\gamma+1}} \right) = \frac{k_s}{R} \left(C_1 + \frac{C_{-1}}{R^2} \right). \tag{32}$$

From (29)–(32), the coefficients B_1 , B_{-1} , C_1 , and C_{-1} can be expressed by A_1 as follows:

$$B_1 = L_1 A_1 \quad B_{-1} = L_{-1} A_1 \quad C_1 = M_1 A_1 \quad C_{-1} = M_{-1} A_1, \tag{33}$$

where

$$\begin{aligned} L_1 &= \frac{R_0^{1-\gamma}}{2} \left(1 + \frac{k_0}{\sqrt{k_r k_\theta}} \right), \\ L_{-1} &= \frac{R_0^{1+\gamma}}{2} \left(1 - \frac{k_0}{\sqrt{k_r k_\theta}} \right), \\ M_1 &= \frac{1}{4k_m} \left[\left(k_m + \frac{k_s}{R} + \gamma k_r \right) \left(1 + \frac{k_0}{\sqrt{k_r k_\theta}} \right) \frac{R^{\gamma-1}}{R_0^{\gamma-1}} + \left(k_m + \frac{k_s}{R} - \gamma k_r \right) \frac{R_0^{\gamma+1}}{R^{\gamma+1}} \left(1 - \frac{k_0}{\sqrt{k_r k_\theta}} \right) \right], \\ M_{-1} &= \frac{R^2}{4k_m} \left[\left(k_m - \frac{k_s}{R} - \gamma k_r \right) \left(1 + \frac{k_0}{\sqrt{k_r k_\theta}} \right) \frac{R^{\gamma-1}}{R_0^{\gamma-1}} + \left(k_m - \frac{k_s}{R} + \gamma k_r \right) \frac{R_0^{\gamma+1}}{R^{\gamma+1}} \left(1 - \frac{k_0}{\sqrt{k_r k_\theta}} \right) \right]. \end{aligned} \tag{34}$$

From (28) and (33), it follows that

$$\begin{aligned} A_1 &= -\frac{q_x^\infty}{Q}, \\ Q &= \frac{1}{4} \left[\left(k_m + \frac{k_s}{R} + \gamma k_r \right) \left(1 + \frac{k_0}{\sqrt{k_r k_\theta}} \right) \frac{R^{\gamma-1}}{R_0^{\gamma-1}} + \left(k_m + \frac{k_s}{R} - \gamma k_r \right) \frac{R_0^{\gamma+1}}{R^{\gamma+1}} \left(1 - \frac{k_0}{\sqrt{k_r k_\theta}} \right) \right]. \end{aligned} \tag{35}$$

From (12), (15), (16), (25)–(27), the overall heat flux fields in the core, fiber and matrix can be expressed as

$$\begin{Bmatrix} q_r^0 \\ q_\theta^0 \end{Bmatrix} = k_0 A_1 \begin{Bmatrix} -\cos \theta \\ \sin \theta \end{Bmatrix} \quad \text{in the core,} \tag{36}$$

$$\begin{Bmatrix} q_r^f \\ q_\theta^f \end{Bmatrix} = \begin{Bmatrix} \gamma k_r \cos \theta \left(\frac{B_{-1}}{r^{\gamma+1}} - B_1 r^{\gamma-1} \right) \\ k_\theta \sin \theta \left(\frac{B_{-1}}{r^{\gamma+1}} + B_1 r^{\gamma-1} \right) \end{Bmatrix} \quad \text{in the fiber,} \tag{37}$$

$$\begin{Bmatrix} q_r^m \\ q_\theta^m \end{Bmatrix} = k_m \begin{Bmatrix} \cos \theta \left(\frac{C_{-1}}{r^2} - C_1 \right) \\ \sin \theta \left(\frac{C_{-1}}{r^2} + C_1 \right) \end{Bmatrix} \quad \text{in the matrix,} \tag{38}$$

where the expression of coefficients $A_1, B_1, B_{-1}, C_1,$ and C_{-1} are shown in (33)–(35).

4. Results and discussion

As an example discussion, take the carbon fiber reinforced epoxy resin as the computational object in this work. The conductivity of the epoxy resin matrix is $k_m = 0.19 \text{ W/mK}$. The unit of the interface thermal constant k_s is W/K . Due to the lack of research on the interface thermal constant of the nanofiber in the existing literature, it is assumed that the ration of the thermal constant of the interface to that of the matrix is a real constant $k_s/k_m = 2 \times 10^{-10} \text{ m}$ according to the theory of surface elasticity [Xiao et al. 2018; Luo and Wang 2009].

The radial and circumferential conductivities of the cylindrically orthotropic fiber are not available and hardly measured by an experiment [Yan et al. 2010]. According to a reasonable assumption by Hasselman et al. [1993], the parameters are taken as $k_r/k_m = 100$ and $k_\theta/k_m = 2.4$ for a radially orthotropic fiber, and $k_r/k_m = 2.4$ and $k_\theta/k_m = 100$ for a circumferentially orthotropic fiber. For the convenience of comparison, choose the parameters with $k_r/k_m = k_\theta/k_m = \sqrt{240}$ for a transversely isotropic fiber [Yan et al. 2010].

Example 1. The variations of the dimensionless heat fluxes along the interfaces S of the fiber are plotted in Figure 2, where $k_m = 0.19 \text{ W/mK}$, $k_s/k_m = 2 \times 10^{-10} \text{ m}$, $R_0/R = 0.1$, $k_0/k_m = 51.2$ and fiber radius $R = 5 \text{ nm}$.

With the increase in angle θ from 0° to 90° , the radial heat flux decreases to zero gradually, while the circumferential heat flux increases from zero monotonously. It is seen that when the radial and circumferential conductivities of the fiber change, it has little effect on the radial heat flux, whereas it has a great effect on circumferential heat flux.

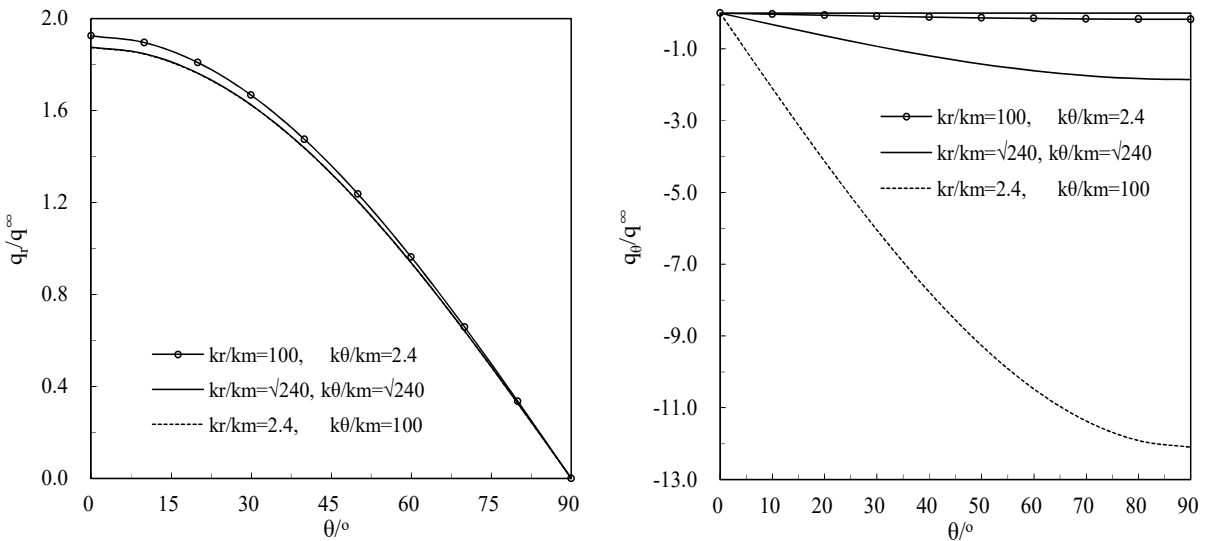


Figure 2. Distributions of the dimensionless heat fluxes on the interfaces S of the fiber: radial heat flux q_r/q_∞ (left) and circumferential heat flux q_θ/q_∞ (right).

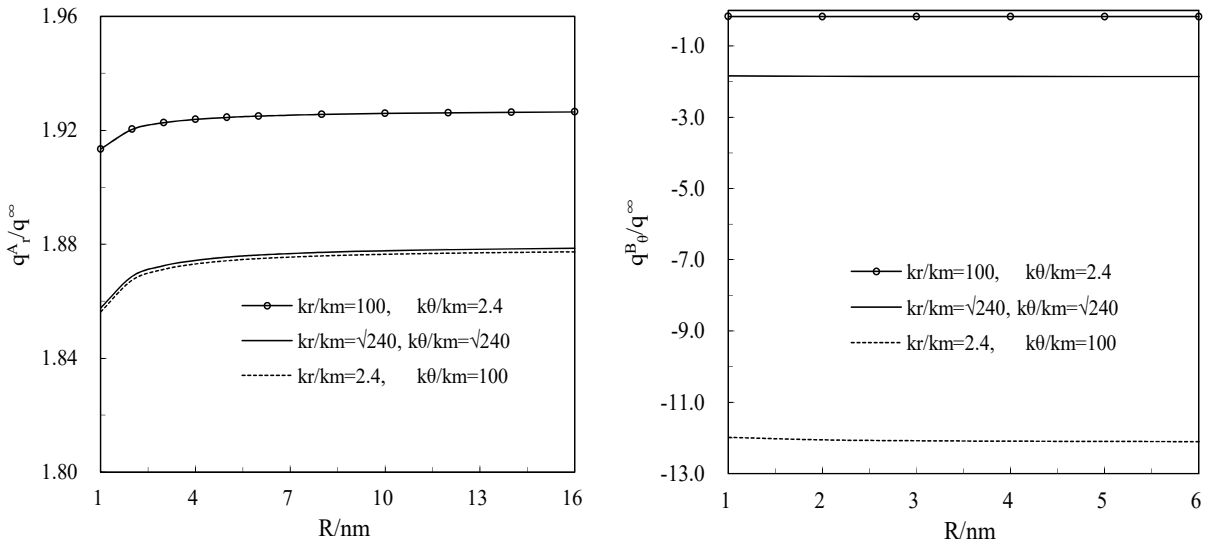


Figure 3. Effects of the size of the fiber on the dimensionless heat fluxes: radial heat flux q_r/q^∞ at point A (left) and circumferential heat flux q_θ/q^∞ at point B (right).

Example 2. The effects of size of the fiber on the dimensionless heat fluxes at point A (maximum radial heat flux on the fiber interface as seen in Figure 2, left) and point B (maximum circumferential heat flux on the fiber interface as seen in Figure 2, right) are depicted in Figure 3, where $k_m = 0.19 \text{ W/mK}$, $k_s/k_m = 2 \times 10^{-10} \text{ m}$, $R_0/R = 0.1$ and $k_0/k_m = 51.2$.

Figure 3 (left) shows that when the size of the fiber is at the nanometer scale, the radial heat flux at point A is size dependent, while the circumferential heat flux at point B has nothing to do with the size of the fiber.

Example 3. The variations of the dimensionless heat fluxes at points A and B with the nondimensional conductivity of the core k_0/k_m are plotted in Figure 4, where $k_m = 0.19 \text{ W/mK}$, $k_s/k_m = 2 \times 10^{-10} \text{ m}$, $R_0/R = 0.1$ and fiber radius $R = 5 \text{ nm}$.

It is seen that with the increase of k_0/k_m , the influence of the conductivity of the core on the radial heat flux at point A is significant when $k_r > k_\theta$, while becomes slight when $k_r < k_\theta$. The change in the conductivity of the core has little effect on the circumferential heat flux at point B on the fiber interface.

Example 4. The variations in the dimensionless heat fluxes at points A and B with the nondimensional radius R_0/R of the core are plotted in Figure 5, where $k_m = 0.19 \text{ W/mK}$, $k_s/k_m = 2 \times 10^{-10} \text{ m}$, $k_0/k_m = 51.2$ and fiber radius $R = 5 \text{ nm}$.

It is seen that the radial and circumferential heat fluxes increase monotonically when the core radius R_0/R increases gradually from 0 to 1. Figure 5 illustrates an interesting phenomenon in which the effect of the core radius on the heat fluxes depends on the cylindrical orthotropy of the fiber. If $k_r \gg k_\theta$, the radial heat flux at point A first increases significantly ($R_0/R < 0.1$), and then slowly tend to a constant value. For the circumferential heat flux at point B, the influence of the core radius can be ignored. If $k_r \ll k_\theta$, the radial heat flux at point A first almost unchanged ($R_0/R < 0.8$), and then drastically increases.

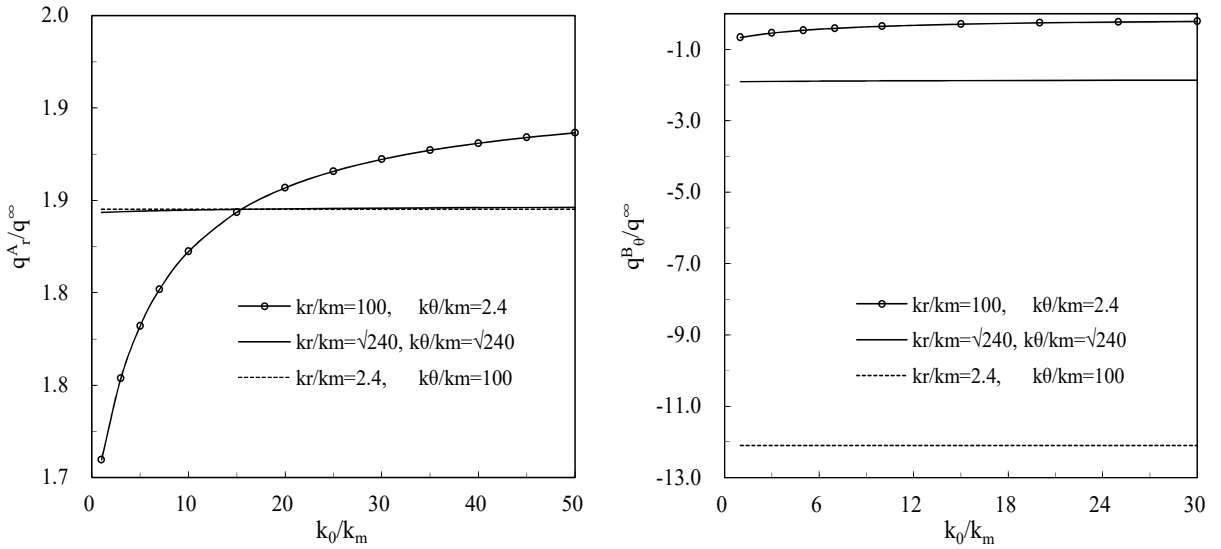


Figure 4. Effects of the nondimensional conductivity of the core k_0/k_m on the dimensionless heat fluxes: radial heat flux q_r/q^∞ at point A (left) and circumferential heat flux q_θ/q^∞ at point B (right).

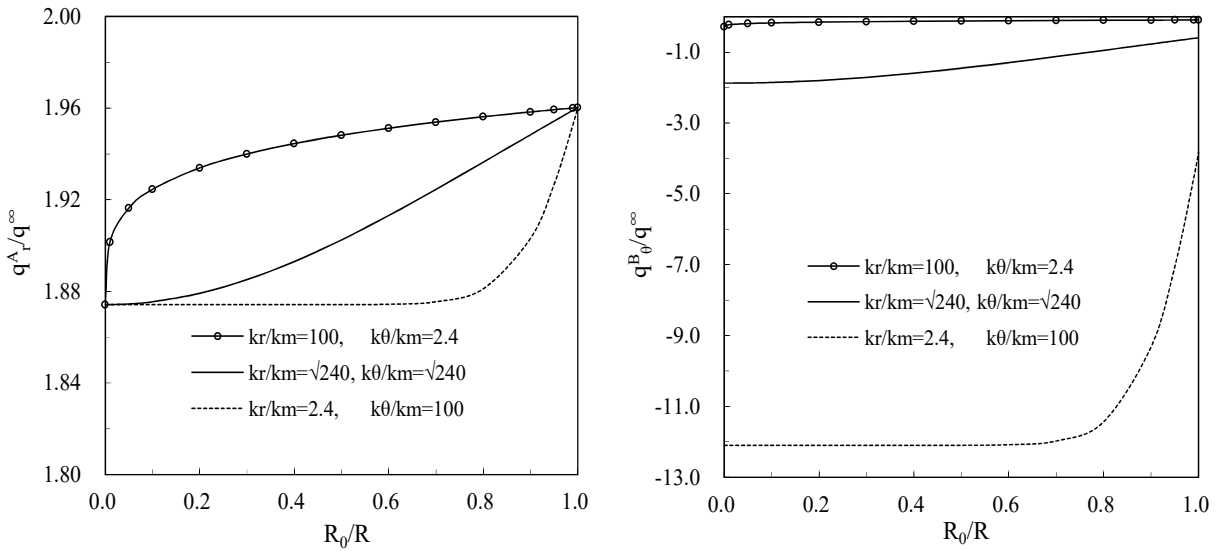


Figure 5. Effects of the nondimensional radius R_0/R of the core on the dimensionless heat fluxes: radial heat flux q_r/q^∞ at point A (left) and circumferential heat flux q_θ/q^∞ at point B (right).

For the circumferential heat flux at point B, the influence of the core radius is slight when $R_0/R < 0.8$, but becomes significant with the increase of R_0/R .

5. Conclusions

The problem of composites reinforced with cylindrically orthotropic nanofiber under two-dimensional steady-state heat conduction is investigated based on the surface theory model and the theory of complex variable elasticity. An analytical solution for the heat flux fields in the nanocomposites is obtained. The effects of fiber size, core thermal conductivity and core radius on the heat flux fields are discussed. The major results are: (a) Changes in the radial and circumferential conductivities of the fiber have little effect on the radial heat flux, but have a great effect on circumferential heat flux. (b) When the size of the fiber is at the nanometer scale, the radial heat fluxes are size dependent and the circumferential heat fluxes shows size independent. (c) The influences of the core thermal conductivity and the core radius on the radial and circumferential heat flux depend on the cylindrical orthotropy of the fiber.

Acknowledgments

This work was supported by the National Natural Science Foundation of China (11302186, 51471146) and the Hebei Province High School Top Young Talent (BJ2014058).

References

- [Alifanov 1994] O. M. Alifanov, *Inverse heat transfer problems*, Springer, New York, 1994.
- [Avery and Herakovich 1986] W. B. Avery and C. T. Herakovich, “Effect of fiber anisotropy on thermal stresses in fibrous composites”, *J. Appl. Mech. (ASME)* **53**:4 (1986), 751–756.
- [Christensen 1994] R. M. Christensen, “Properties of carbon fibers”, *J. Mech. Phys. Solids* **42**:4 (1994), 681–695.
- [DeValve and Pitchumani 2013] C. DeValve and R. Pitchumani, “Experimental investigation of the damping enhancement in fiber-reinforced composites with carbon nanotubes”, *Carbon* **63** (2013), 71–83.
- [Duan and Karihaloo 2007] H. L. Duan and B. L. Karihaloo, “Thermo-elastic properties of heterogeneous materials with imperfect interfaces: generalized Levin’s formula and Hill’s connections”, *J. Mech. Phys. Solids* **55**:5 (2007), 1036–1052.
- [Frankel et al. 2008] J. I. Frankel, M. Keyhani, R. V. Arimilli, and J. Wu, “A new multidimensional integral relationship between heat flux and temperature for direct internal assessment of heat flux”, *Z. Angew. Math. Phys.* **59**:5 (2008), 869–888.
- [Frankel et al. 2010] J. I. Frankel, M. Keyhani, B. Elkins, and R. V. Arimilli, “A new anisotropic, two-dimensional, transient heat flux-temperature integral relationship for half-space diffusion”, *J. Appl. Math. Mech.* **90**:2 (2010), 161–170.
- [Gori and Corasaniti 2014] F. Gori and S. Corasaniti, “Effective thermal conductivity of composites”, *Int. J. Heat Mass Transf.* **77** (2014), 653–661.
- [Gounni and Alami 2017] A. Gounni and M. E. Alami, “The optimal allocation of the PCM within a composite wall for surface temperature and heat flux reduction: an experimental approach”, *Appl. Therm. Eng.* **127** (2017), 1488–1494.
- [Gurtin and Murdoch 1975] M. E. Gurtin and A. I. Murdoch, “A continuum theory of elastic material surfaces”, *Arch. Ration. Mech. Anal.* **57**:4 (1975), 291–323.
- [Gurtin and Murdoch 1978] M. E. Gurtin and A. I. Murdoch, “Surface stress in solids”, *Int. J. Solids Struct.* **14**:6 (1978), 431–440.
- [Gurtin et al. 1998] M. E. Gurtin, J. Weissmüller, and F. Larché, “A general theory of curved deformable interfaces in solids at equilibrium”, *Philos. Mag. A* **78**:5 (1998), 1093–1109.
- [Györy and Márkus 2014] E. Györy and F. Márkus, “Size dependent thermal conductivity in nano-systems”, *Thin Solid Films* **565** (2014), 89–93.
- [Hashin 1990] Z. Hashin, “Thermoelastic properties and conductivity of carbon/carbon fiber composites”, *Mech. Mater.* **8**:4 (1990), 293–308.

- [Hasselman et al. 1993] D. P. H. Hasselman, K. Y. Donaldson, and J. R. Thomas Jr, “Effective thermal conductivity of uniaxial composite with cylindrically orthotropic carbon fibers and interfacial thermal barrier”, *J. Compos. Mater.* **27**:6 (1993), 637–644.
- [Hattiangadi and Siegmund 2005] A. Hattiangadi and T. Siegmund, “A numerical study on interface crack growth under heat flux loading”, *Int. J. Solids Struct.* **42**:24–25 (2005), 6335–6355.
- [Khan et al. 2010] S. U. Khan, A. Munir, R. Hussain, and J.-K. Kim, “Fatigue damage behaviors of carbon fiber-reinforced epoxy composites containing nanoclay”, *Compos. Sci. Technol.* **70**:14 (2010), 2077–2085.
- [Knott and Herakovich 1991] T. W. Knott and C. T. Herakovich, “Effect of fiber orthotropy on effective composite properties”, *J. Compos. Mater.* **25**:6 (1991), 732–759.
- [Lee et al. 2012] H.-L. Lee, W.-J. Chang, S.-H. Sun, and Y.-C. Yang, “Estimation of temperature distributions and thermal stresses in a functionally graded hollow cylinder simultaneously subjected to inner-and-outer boundary heat fluxes”, *Compos. B Eng.* **43**:2 (2012), 786–792.
- [Li et al. 2017] Y. Li, S. Cai, and X. Huang, “Multi-scaled enhancement of damping property for carbon fiber reinforced composites”, *Compos. Sci. Technol.* **143** (2017), 89–97.
- [Luo and Wang 2009] J. Luo and X. Wang, “On the anti-plane shear of an elliptic nano inhomogeneity”, *Eur. J. Mech. A Solids* **28**:5 (2009), 926–934.
- [Machrafi 2016] H. Machrafi, “An extended thermodynamic model for size-dependent thermoelectric properties at nanometric scales: application to nanofilms, nanocomposites and thin nanocomposite films”, *Appl. Math. Model.* **40**:3 (2016), 2143–2160.
- [Muskhelishvili 1953] N. I. Muskhelishvili, *Some basic problems of the mathematical theory of elasticity*, Noordhoff, Groningen, 1953.
- [Orlande 2011] H. R. B. Orlande, “Inverse heat transfer problems”, *Head Transf. Eng.* **32**:9 (2011), 715–717.
- [Peng et al. 2017] M. Peng, Y. Zhou, G. Zhou, and H. Yao, “Triglycidyl para-aminophenol modified montmorillonites for epoxy nanocomposites and multi-scale carbon fiber reinforced composites with superior mechanical properties”, *Compos. Sci. Technol.* **148** (2017), 80–88.
- [Rodríguez and Cabeza 1999] A. C. Rodríguez and J. M. G. Cabeza, “Effect of cylindrically orthotropic carbon fibers with transversely isotropic core on effective thermal conductivity of unidirectional composites”, *J. Compos. Mater.* **33**:11 (1999), 984–1001.
- [Rylko 2015] N. Rylko, “Edge effects for heat flux in fibrous composites”, *Comput. Math. Appl.* **70**:10 (2015), 2283–2291.
- [Shi et al. 2013] S. Shi, J. Liang, and G. Lin, G. Fang, “High temperature thermomechanical behavior of silica-phenolic composite exposed to heat flux environments”, *Compos. Sci. Technol.* **87**:9 (2013), 204–209.
- [Sobolev 2017] S. L. Sobolev, “Discrete space-time model for heat conduction: application to size-dependent thermal conductivity in nano-films”, *Int. J. Heat Mass Transf.* **108** (2017), 933–939.
- [Stokes-Griffin and Compston 2016] C. M. Stokes-Griffin and P. Compston, “An inverse model for optimisation of laser heat flux distributions in an automated laser tape placement process for carbon-fibre/PEEK”, *Compos. A Appl. Sci. Manuf.* **88** (2016), 190–197.
- [Wang et al. 2012] W. G. Wang, B. L. Xiao, and Z. Y. Ma, “Evolution of interfacial nanostructures and stress states in Mg matrix composites reinforced with coated continuous carbon fibers”, *Compos. Sci. Technol.* **72**:2 (2012), 152–158.
- [Xiao et al. 2018] J. Xiao, Y. Xu, and F. Zhang, “An analytical method for predicting the effective transverse thermal conductivity of nano coated fiber composites”, *Compos. Struct.* **189** (2018), 553–559.
- [Yan et al. 2010] P. Yan, C. P. Jiang, and F. Song, “A complex variable solution of two-dimensional heat conduction of composites reinforced with periodic arrays of cylindrically orthotropic fibers”, *Comput. Mater. Sci.* **50**:2 (2010), 704–713.
- [Yang and Chang 2006] Y.-C. Yang and W.-J. Chang, “Simultaneous inverse estimation for boundary heat and moisture fluxes of a double-layer annular cylinder with interface resistance”, *Appl. Math. Comput.* **176**:2 (2006), 594–608.
- [Yang et al. 2010] Y.-C. Yang, S.-S. Chu, W.-J. Chang, and T.-S. Wu, “Estimation of heat flux and temperature distributions in a composite strip and homogeneous foundation”, *Int. Commun. Heat Mass* **37**:5 (2010), 495–500.
- [Yang et al. 2013] Y.-C. Yang, W.-L. Chen, H.-M. Chou, and J. L. L. Salazar, “Inverse hyperbolic thermoelastic analysis of a functionally graded hollow circular cylinder in estimating surface heat flux and thermal stresses”, *Int. J. Heat Mass Transf.* **60** (2013), 125–133.

[Yin et al. 2008] H. M. Yin, G. H. Paulino, W. G. Buttlar, and L. Z. Sun, “Heat flux field for one spherical inhomogeneity embedded in a functionally graded material matrix”, *Int. J. Heat Mass Transf.* **51**:11 (2008), 3018–3024.

Received 27 May 2018. Revised 2 Sep 2018. Accepted 28 Sep 2018.

JUNHUA XIAO: xiaojunhua@ysu.edu.cn

Key Laboratory of Mechanical Reliability for Heavy Equipments and Large Structures of Hebei Province, Yanshan University, Qinhuangdao 066004, China

YAOLING XU: xylysu@163.com

Key Laboratory of Mechanical Reliability for Heavy Equipments and Large Structures of Hebei Province, Yanshan University, Qinhuangdao 066004, China

FUCHENG ZHANG: zfc@ysu.edu.cn

State Key Laboratory of Metastable Materials Science and Technology, Yanshan University, Qinhuangdao 066004, China

JOURNAL OF MECHANICS OF MATERIALS AND STRUCTURES

msp.org/jomms

Founded by Charles R. Steele and Marie-Louise Steele

EDITORIAL BOARD

ADAIR R. AGUIAR	University of São Paulo at São Carlos, Brazil
KATIA BERTOLDI	Harvard University, USA
DAVIDE BIGONI	University of Trento, Italy
MAENGHYO CHO	Seoul National University, Korea
HUILING DUAN	Beijing University
YIBIN FU	Keele University, UK
IWONA JASIUK	University of Illinois at Urbana-Champaign, USA
DENNIS KOCHMANN	ETH Zurich
MITSUTOSHI KURODA	Yamagata University, Japan
CHEE W. LIM	City University of Hong Kong
ZISHUN LIU	Xi'an Jiaotong University, China
THOMAS J. PENCE	Michigan State University, USA
GIANNI ROYER-CARFAGNI	Università degli studi di Parma, Italy
DAVID STEIGMANN	University of California at Berkeley, USA
PAUL STEINMANN	Friedrich-Alexander-Universität Erlangen-Nürnberg, Germany
KENJIRO TERADA	Tohoku University, Japan

ADVISORY BOARD

J. P. CARTER	University of Sydney, Australia
D. H. HODGES	Georgia Institute of Technology, USA
J. HUTCHINSON	Harvard University, USA
D. PAMPLONA	Universidade Católica do Rio de Janeiro, Brazil
M. B. RUBIN	Technion, Haifa, Israel

PRODUCTION production@msp.org


SILVIO LEVY Scientific Editor

See msp.org/jomms for submission guidelines.

JoMMS (ISSN 1559-3959) at Mathematical Sciences Publishers, 798 Evans Hall #6840, c/o University of California, Berkeley, CA 94720-3840, is published in 10 issues a year. The subscription price for 2018 is US \$615/year for the electronic version, and \$775/year (+\$60, if shipping outside the US) for print and electronic. Subscriptions, requests for back issues, and changes of address should be sent to MSP.

JoMMS peer-review and production is managed by EditFLOW[®] from Mathematical Sciences Publishers.

PUBLISHED BY

 **mathematical sciences publishers**
nonprofit scientific publishing

<http://msp.org/>

© 2018 Mathematical Sciences Publishers

- Prediction of springback and residual stress of a beam/plate subjected to three-point bending** **QUANG KHOA DANG, PEI-LUN CHANG, SHIH-KANG KUO and DUNG-AN WANG** **421**
- Characterization of CNT properties using space-frame structure** **MUHAMMAD ARIF and JACOB MUTHU** **443**
- Analytical approach to the problem of an auxetic layer under a spatially periodic load** **HENRYK KAMIŃSKI and PAWEŁ FRITZKOWSKI** **463**
- Stability and nonplanar postbuckling behavior of current-carrying microwires in a longitudinal magnetic field** **YUANZHUO HONG, LIN WANG and HU-LIANG DAI** **481**
- Three-dimensional Trefftz computational grains for the micromechanical modeling of heterogeneous media with coated spherical inclusions** **GUANNAN WANG, LEITING DONG, JUNBO WANG and SATYA N. ATLURI** **505**
- Uniform stress resultants inside two nonelliptical inhomogeneities in isotropic laminated plates** **XU WANG, LIANG CHEN and PETER SCHIAVONE** **531**
- An analytical solution for heat flux distribution of cylindrically orthotropic fiber reinforced composites with surface effect** **JUNHUA XIAO, YAOLING XU and FUCHENG ZHANG** **543**
- Strain gradient fracture of a mode III crack in an elastic layer on a substrate** **JINE LI and BAOLIN WANG** **555**
- Growth-induced instabilities of an elastic film on a viscoelastic substrate: analytical solution and computational approach via eigenvalue analysis** **IMAN VALIZADEH, PAUL STEINMANN and ALI JAVILI** **571**
- Application of the hybrid complex variable method to the analysis of a crack at a piezoelectric-metal interface** **VOLODYMYR GOVORUKHA and MARC KAMLAH** **587**